

## Microstructure based upper shelf Charpy toughness prediction of HSLA steels

Florian Thönnessen<sup>1,a</sup>, Sebastian Münstermann<sup>1,b</sup>, Wolfgang Bleck<sup>1,c</sup>,  
Philippe Thibaux<sup>2,d</sup>, Martin Liebeherr<sup>2,e</sup>, Thomas Schramm<sup>3,f</sup>

<sup>1</sup> Department of Ferrous Metallurgy, RWTH Aachen University,  
Intzestrasse 1, 52070 Aachen, Germany

<sup>2</sup> ArcelorMittal R&D Industry Gent, OCAS NV, Pres.J.F. Kennedylaan 3, 9060 Zelzate, Belgium

<sup>3</sup> ArcelorMittal Hamburg GmbH, Dradenaustraße 33, 21129 Hamburg, Germany

<sup>a</sup>florian.thoennessen@iehk.rwth-aachen.de, <sup>b</sup>sebastian.muenstermann@iehk.rwth-aachen.de,  
<sup>c</sup>wolfgang.bleck@iehk.rwth-aachen.de, <sup>d</sup>Philippe.Thibaux@arcelormittal.com,  
<sup>e</sup>martin.liebeherr@arcelormittal.com, <sup>f</sup>thomas.schramm@arcelormittal.com

**Keywords:** quantitative fractography, quantitative metallography, Focussed Ion Beam, GTN model, damage modelling, Charpy toughness prediction.

**Abstract.** Three high strength low alloy steels with bainitic microstructures and high internal cleanliness level have been investigated. All three steels have similar chemical compositions and strength properties, but toughness properties vary in transition temperature as well as in upper shelf values. It is the aim of this work to explain different upper shelf toughness properties by the results of microstructural investigations in a first step and then, in a second step, to use the obtained data for numerical prediction of toughness values. The investigations show that in the selected high strength low alloy steels of highest cleanliness, only few primary voids nucleate at non-metallic inclusions at the onset of plastic deformation, whereas a second population of significantly smaller voids is assumed to nucleate during straining. Zones of finest precipitated iron-carbides are assumed to be the main secondary voids nucleating microstructural constituent. The role of Martensite/Austenite-constituents in this process can be neglected. The microstructural data obtained are used as parameters for the Gurson-Tvergaard-Needleman (GTN) damage model. Further model parameters are derived experimentally and numerically. The GTN model is employed to pre-calculate upper shelf Charpy impact toughness with good agreement to experimental results.

### Introduction

High strength low alloy (HSLA) steels must have excellent toughness properties to avoid brittle failure and to ensure good crack arrest properties. Modern HSLA steels with high internal cleanliness level and bainitic microstructures fulfil these demands. For future materials improvement a quantitative description of ductile and brittle failure behaviour and its relationship to microstructure is evident.

On the microstructural level ductile failure is controlled by strain hardening and by nucleation, growth and coalescence of voids. In steels of highest cleanliness, only few primary voids nucleate at non-metallic inclusions at the onset of plastic deformation, whereas a second population of significantly smaller voids is assumed to nucleate during straining. A correlation of secondary voids nucleation sites to corresponding microstructural constituents is not yet known for such steels.

The aim of this work is developing a tool to predict toughness of HSLA steels. This tool shall be initially based on quantifiable mechanical and microstructural analysis. As the continuum damage mechanics model by Gurson-Tvergaard-Needleman (GTN) is able to link failure causing and quantifiable microstructural constituents with initial void growth, void nucleation and void coalescence, this model is chosen to describe the upper shelf behaviour [1,2,3,4,5]. Based on mechanical and microstructural investigations an individual parameter set will be defined for each steel and upper shelf toughness properties will be predicted numerically. A fitting of the model parameters should be avoided as the relation between microstructure and toughness would be lost otherwise. Besides the flow curve, altogether nine parameters of the GTN model have to be quantified for damage modelling in case of quasistatic, isothermal loading: initial void volume  $f_0$ , volume fraction of new voids  $f_N$ , characteristic strain of secondary void nucleation  $\epsilon_N$ , standard deviation of strain controlled secondary void nucleation  $S_N$ , critical void volume fraction  $f_C$ , model parameters  $q_1, q_2, q_3$  and acceleration factor  $\kappa$  [6]. To respect adiabatic conditions further model parameters have to be considered [7].

### Materials

Three thermomechanical treated and coiled HSLA heavy plate steels are investigated on mechanical properties and microstructure. The thickness of steels A and B is 18 mm, that of steel C is 20 mm. The chemical compositions (Table 1) and strength properties (Fig. 1) of these steels are nearly identical, whereas the toughness properties (Fig. 2) are different. Steel C shows the highest upper shelf values and has the lowest transition temperature. Steel A shows contrary behaviour.

Element	Steel A	Steel B	Steel C
C	0.056	0.064	0.045
Mn	1.46	1.43	1.43
S	<0.001	<0.001	<0.001
Others	MoNiNbTi		

Table 1: Chemical composition of investigated steels, mass contents in %.

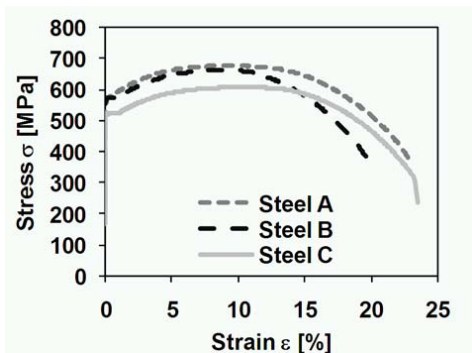


Figure 1: Tensile test results at room temperature.

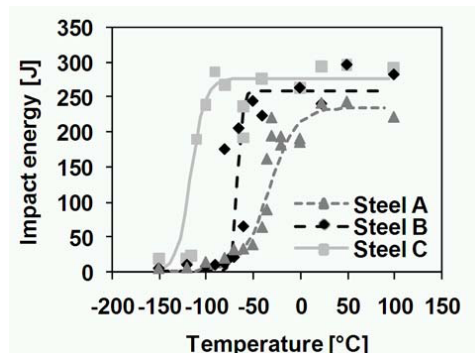


Figure 2: Charpy impact toughness properties in dependence of temperature.

### Microstructural characterisation

In a first step qualitative fractographic investigations on ductile fracture surfaces are carried out by scanning electron microscopy (SEM) in order to identify different populations of voids (Fig. 3). All three steels fail by growth of big, primary voids with a size of approximately 20-30  $\mu\text{m}$  and nucleation of significant smaller secondary voids with a size of approximately 2-5  $\mu\text{m}$ . In some primary voids particles can be identified. By wavelength dispersive X-ray diffraction (WDX) analysis the nature of these particles is identified. All particles are analysed to be conglomerates consisting of Al, Ca, Mn, O, S and rarely Ti, that is why they can be classified as inclusions originate from the metallurgical process chain.

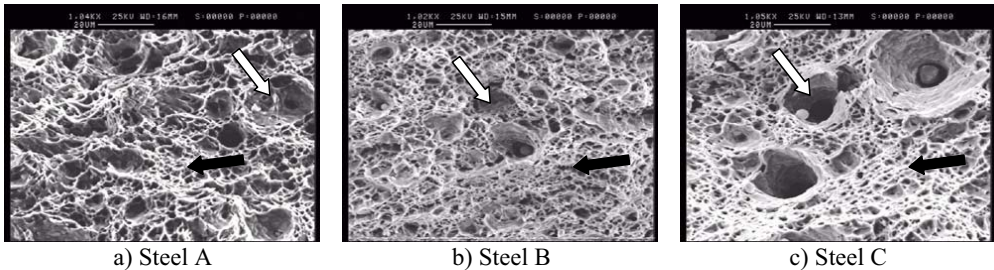


Figure 3 a)-c): Ductile fracture surfaces by SEM, white arrows indicate primary voids, black arrows indicate secondary voids, magnification 1000:1.

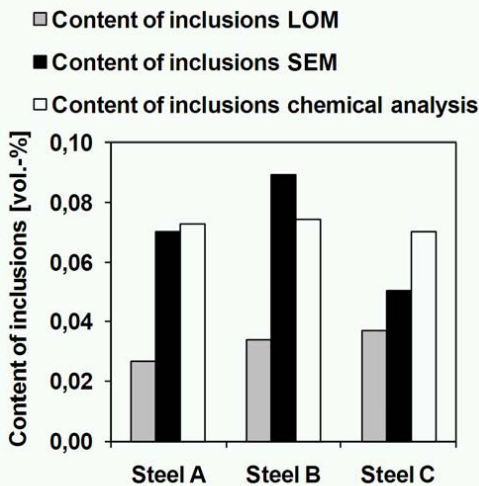


Figure 4: Determination of inclusions volume content by LOM, SEM and chemical analysis.

Consequently a quantitative analysis of inclusions has been carried out (Fig. 4). The content of inclusions has been analysed on polished, but unetched samples by light optical microscopy (LOM) and by SEM. In the LOM the magnification has been 1000:1, in the SEM 1500:1. Totally an area of approximately 50mm<sup>2</sup> is analysed in the LOM. An area of 1,8mm<sup>2</sup> is analysed in the SEM. To determine the chemistry of inclusions, the SEM investigations are performed together with a WDX analysis. In accordance to the above described analysis of primary voids inducing particles, all analysed inclusions consist of Al, Ca, Mn, O, S and Ti. Based on the simplification that only particles of the type Al<sub>2</sub>O<sub>3</sub>, CaO, MnS and TiN are responsible for initial void growth, the volume content has been calculated by taken the chemical analysis, the mole mass and the

chemical density into account. Due to higher precision, SEM and the estimation on chemical analysis give highest values for the inclusion amount. As the influence of Ti-containing particles on initial void growth is slightly overestimated by SEM and by inclusion analysis based on chemical composition, the inclusion content determined by LOM is taken as initial void volume  $f_0$  in the numerical part of this work.

As the volume of activated matrix material by WDX analysis is much bigger than a single secondary void, a direct identification of secondary voids causing particles is not possible by WDX analysis of ductile fracture surfaces. A first step to identify these particles has been carried out by a qualitative metallographic analysis. Representative for all investigated steels, Fig. 5 shows the bainitic microstructure by HNO<sub>3</sub> etching. The microstructure consists of acicular ferrite with bainite packages, in Fig. 5 indicated as island-type black spots. Fig. 6 presents an enlarged view on a bainite package with martensite/austenite (M/A)-constituent. The nature of bainite packages is equal for all three steels. These zones consist of finest precipitated iron-carbides, originally formed from carbon enriched austenite. Besides this, there exist M/A-constituents that have not been transformed completely after  $\alpha$ - $\gamma$ -phase transformation. In the following these two microstructural constituents, bainite packages and M/A-constituents, are assumed to be responsible for secondary voids growth.

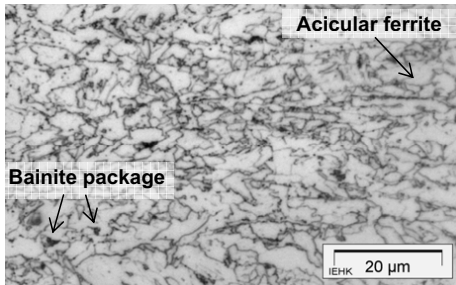


Figure 5: HNO<sub>3</sub> etching of Steel A in rolling direction, magnification 1000:1.

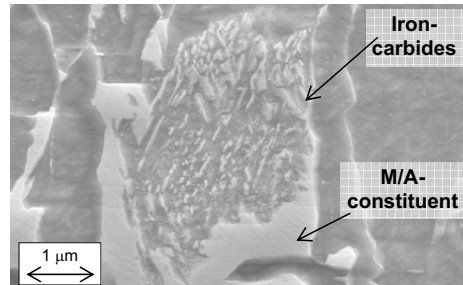


Figure 6: Bainite package of Steel A in SEM after HNO<sub>3</sub> etching, magnification 42000:1.

To quantify bainite packages volume content and number, colour tint etchings with sodium-picrat are performed (Fig 7). This etching method enables an isolated presentation of carbides [8]. To quantify M/A-constituents, colour tint etchings after Klemm [8,9] are carried out (Fig. 9). Here, austenite containing phases appear white. 10 pictures in magnification of 1.000:1 in rolling direction of sodium-picrat and Klemm etched microstructures have been taken at sub-surface, quarter- and half-thickness. Content and number of the phases are analysed with the digital imaging software analySIS®, see Fig. 8 and Fig. 10. The content of bainite packages is constant over thickness for each steel, except the position subsurface of Steel C. It goes slightly along with the carbon content. The higher the carbon content is, the higher is the amount of bainite packages. The content of M/A-constituents is considerable lower. Due to segregation effects, this content varies over thickness. Centralised, it is shown that the amount of bainite packages and M/A-constituents can be quantified by appropriate etching methods and following imaging analysis.

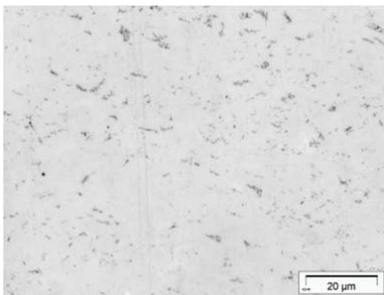


Figure 7: Sodium-picrat etching of Steel A, dark spots indicate bainite packages, magnification 1000:1.

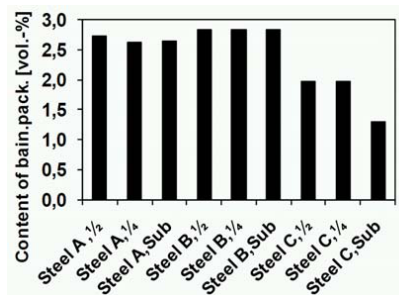


Figure 8: Determination of bainite packages volume content by image analysis of sodium-picrat etchings.

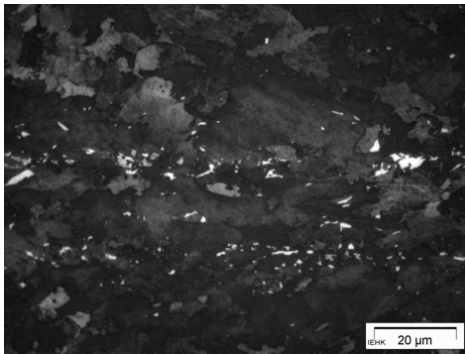


Figure 9: Klemm etching of Steel A in rolling direction, white islands indicate M/A-constituents, magnification 1000:1.

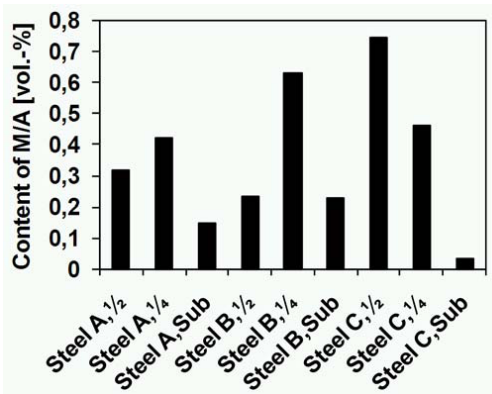


Figure 10: Determination of M/A-constituents volume content by image analysis of Klemm etchings.

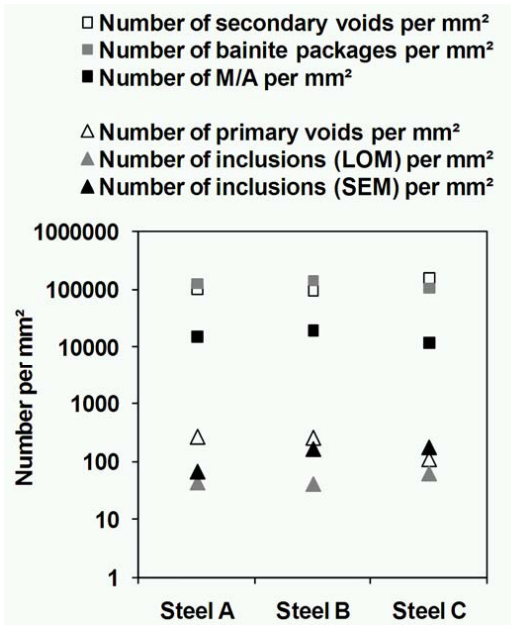


Figure 10: Correlation of number of primary and secondary voids with corresponding microstructural constituents.

A quantitative evaluation of influences on ductile failure by different types of microstructural constituents is performed by correlating results from above shown analysis with quantitative fractography methods (Fig. 10). Besides the volume content, also the number of particles has been determined by image analysis. The number and type of voids have been analysed by quantification of ductile Charpy fracture surfaces. Therefore, per steel 10 pictures have been taken in a SEM, and every picture has been hand copied on a transparency. Afterwards, the fracture surface has been quantified. The results have been the diameter of each void and the number of voids per mm<sup>2</sup>. Voids have been classified into primary voids, if larger than 11 μm, and secondary voids, if smaller than 11 μm. Voids smaller than 0,5 μm have not been taken into account, as these voids are regarded as pixel failures during image analysis. Fig. 10 shows that the number of inclusions fits well with the number of primary voids. Likewise the number of bainite packages fits well with the number of

secondary voids. The role of M/A-constituents can be neglected in the process of secondary voids nucleation.

A qualitative link between bainite packages and/or M/A-constituents and secondary voids growth is performed in two different ways. Firstly, etchings with sodium-picrat have been carried out on interrupted notched tensile sample (Fig. 11). Indicated with arrows, nucleation of new voids is observed in bainite packages.

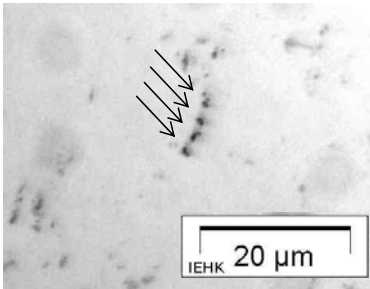
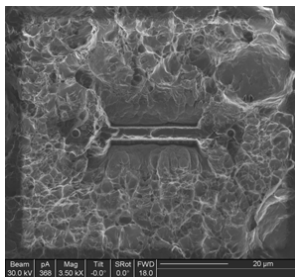
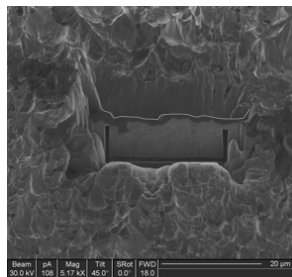


Figure 11: sodium-picrat etching on interrupted notched tensile tests of Steel C, arrows indicate void nucleation in bainite packages, magnification 1000:1.

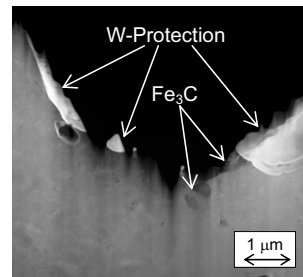
A second possibility is given by the focussed ion beam (FIB) preparation technology for transmission electron microscopy (TEM) investigations. The FIB instrument is similar to a SEM, except that the beam that is rastered over the sample is an ion beam rather than an electron beam. Usually a Gallium-ion beam is used. Secondary electrons are generated by the interaction of the ion beam with the sample surface and can be used to obtain high-spatial-resolution images [10]. Here, this preparation technology for TEM analysis has been employed to prepare a lamella consisting of several secondary voids with a spatial accuracy of within 100 nm (Fig. 12). Before cutting, a tungsten line is deposited on the area of interest to protect the top of the specimen [11]. Both, FIB and TEM investigations are performed at Central Facility for Electron Microscopy of RWTH Aachen University. One single secondary void is analysed in TEM combined with energy dispersive X-ray (EDX) analysis. An accumulation of cementite is identified at the ground of the secondary void, this leads to the conclusion that cementite is responsible for secondary voids nucleation.



a) SEM: top view on lamella before lift-out.



b) SEM: view on lamella 70° tilted before lift out.



c) TEM: secondary void ground.

Figure 12 a)- c): Preparation of one lamella taken out of a ductile Charpy fracture surface from Steel B by FIB technology for TEM investigations, SEM magnification 5000:1, TEM magnification 20000:1.

For the numerical part of this work, the volume of secondary voids  $f_N$  is linked to the amount of iron-carbides and M/A-constituents.

### Charpy impact toughness prediction

The GTN model is taken to pre-calculate upper shelf Charpy toughness. The provided flow curves are extrapolated using the approach by Bridgman [12]. The parameters  $f_0$  and  $f_N$  are analysed as described in the chapter before.  $\epsilon_N$  is analysed by applying the direct current potential drop method on single edge notched bend samples. The procedure, applied on notched tensile samples, is described in [6].  $\epsilon_N$  is analysed as 0.4 for Steel A, 0.3 for Steel B and 0.3 for Steel C. As commonly used, the corresponding standard deviation is 0,1 [13]. Following the suggestion of Tvergaard and Needleman, the model parameters  $q_1$ ,  $q_2$  and  $q_3$  are chosen to be  $q_1 = 1.5$ ,  $q_2 = 1.0$  and  $q_3 = 2.25$ . The critical void volume fraction  $f_C$  is analysed by unit cell simulations, explained in [14]. Based on

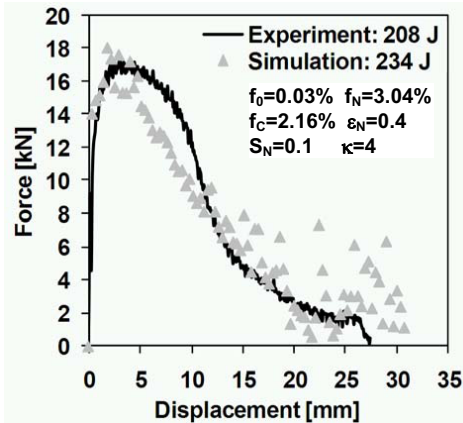


Figure 13: 3D simulation of an instrumented Charpy test of Steel A.

numerical and experimental upper shelf behaviour is shown.

## Conclusions

Three HSLA steels with bainitic microstructure and high purity degree have been investigated on mechanical properties and microstructure. The microstructural data obtained are used as parameters for the GTN model. Further model parameters are derived experimentally and numerically. This damage mechanics approach is employed to predict upper shelf Charpy impact toughness. Based on the above presented results, conclusions can be drawn as follows:

- In HSLA steels with high internal cleanliness level and bainitic microstructures ductile damage is controlled by two populations of voids: growth of initial voids caused by metallurgical induced inclusions and nucleation of new voids. These significant smaller voids nucleate at zones of finest precipitated iron carbides, showed by applying FIB technology for TEM investigations on ductile fracture surfaces.
- The quantification of primary voids causing metallurgical inclusions can be performed either by simple estimation of inclusion volume content based on chemical composition or by purity degree investigations carried out in optical and electron microscope.
- After selecting an appropriate etching method in combination with imaging analysing software, secondary voids inducing microstructural constituents can be quantified. An appropriate etching method is defined as a method that is able to mark secondary voids inducing microstructural constituents isolated from other microstructural features.
- By quantifying ductile fracture surfaces the quantitative analysis of ductile damage causing microstructural constituents can be verified by comparison of number of primary and secondary voids with corresponding microstructural components. Currently this analysis is very time-consuming due to large manual work. An image analysis system either based on differences in grey-scales of SEM pictures or contour lines taken on ductile fracture surfaces could reduce the analysis time.

- As a basic principle the GTN damage mechanics approach is able to predict upper shelf Charpy impact toughness with good agreement to experimental results. Model parameters can be derived by quantitative metallographic investigations, experiments and numerical methods. A fitting of microstructure linked model parameters for better agreement between experiments and simulations is not necessary. Considering that ductile damage causing microstructural constituents are analysed, variations in microstructure and its influences on impact toughness can be pre-calculated numerically. Currently the determination of model parameters is quite extensive. A parameter study could identify strong and weak parameters, so that complex analysis methods should concentrate on the determination of strong parameters.

### Acknowledgements

The presented research results are generated in a project funded by ArcelorMittal R&D Industry Gent, OCAS NV, which are gratefully acknowledged for the support.

### Literature

- [1] A.L. Gurson: J. Engn. Mater. Tech., Vol. 99 (1977), p. 2
- [2] V. Tvergaard: Int. J. Fract., Vol. 18 (1982), p. 237
- [3] V. Tvergaard, A. Needleman: Acta metall., Vol. 32 (1984), No. 1, p. 157
- [4] A. Needleman, V. Tvergaard: J. Mech. Phys. Solids, Vol. 35 (1987), p. 151
- [5] V. Tvergaard, A. Needleman: J. Mech. Phys. Solids, Vol. 40 (1992), No. 2, p. 447
- [6] S. Münstermann, U. Prah, W. Bleck: Steel Research Int., Vol. 78 (2007), No. 3, p. 224
- [7] J. Pan, M. Saje, A. Needleman: Int. J. Fract. Vol 21 (1983), p. 261
- [8] M. Beckert, H. Klemm, in: *Handbuch der metallographischen Ätzverfahren*, 4th Edition, edited by VEB Deutscher Verlag für Grundstoffindustrie, Leipzig, (1985)
- [9] J. Angeli, A. Kneissel, E. Füreder: Prakt. Met. Sonderband Vol. 36 (2004), p. 231
- [10] C.A. Volkert, A.M. Minor: MRS Bulletin, Vol. 32 (2007), No. 5, p. 389
- [11] J. Mayer, L.A. Giannuzzi, T. Kamino, J. Michael, MRS Bulletin, Vol. 32 (2007), No. 5, p. 400
- [12] P.W. Bridgman: Transaction of the A. S. M. Vol. 32 (1944), p. 553
- [13] M. Springmann, M. Kuna: Comp. Mat. Sci., 32 (2005), p. 544
- [14] D. Steglich, in: *Bestimmung von mikrostrukturellen Parametern in Schädigungsmodellen für duktile Materialien*, Dr.-Ing. Diss. TU Berlin, edited by Technical Report GKSS 99/e723, (1999)